Aggregation of Poly(ethylene oxide)−Poly(propylene oxide) Block Copolymers in Aqueous Solution: DPD Simulation Study

Xiaorong Cao, Guiying Xu,* Yiming Li, and Zhiqing Zhang

Key Laboratory of Colloid and Interface Chemistry (Shandong University), Ministry of Education, Jinan 250100, P. R. China

Received: July 4, 2005; In Final Form: September 7, 2005

The dissipative particle dynamics (DPD) simulation method was applied to simulate the aggregation behavior of three block copolymers, $(EO)_{16}(PO)_{18}$, $(EO)_8(PO)_{18}(EO)_8$, and $(PO)_9(EO)_{16}(PO)_9$, in aqueous solutions. The results showed that the size of the micelle increased with increasing concentration. The diblock copolymer $(EO)_{16}(PO)_{18}$ would form an intercluster micelle at a certain concentration range, besides the traditional aggregates (spherical micelle, cylindrical micelle, and lamellar phase); while the triblock copolymer $(EO)_8(PO)_{18}(EO)_8$ would form a spherical micelle, cylindrical micelle, and lamellar phase with increasing concentration, and $(PO)_9(EO)_{16}(PO)_9$ would form intercluster aggregates, as well as a spherical micelle and gel. New mechanisms were given to explain the two kinds of intercluster micelle formed by the different copolymers. It is deduced from the end-to-end distance that the morphologies of the diblock copolymer and triblock copolymer with hydrophilic ends were more extendible than the triblock copolymer with hydrophobic ends.

1. Introduction

Poly(ethylene oxide)−poly(propylene oxide) block copolymers are an important class of amphiphilic molecules whose physicochemical properties have been studied by many researchers.[1−6] Attention arises from both their interesting behavior in self-assembly and their wide application in detergency, formulation of cosmetics dispersion stabilization, lubrication, inks, pharmaceuticals, bioprocess, separations and synthesis of nanoparticles, and others. The action of block copolymers depends strongly on their aggregation in the system. It is well-known that block copolymers have the ability to form micelle, bicontinuous, hexagonal, and lamellar phases. There are several factors contributing to the aggregate morphology, such as temperature, the length ratio of each block, the concentration and structure (i.e., relative block size and block sequence) of the copolymer,[7,8] and others discussed in literature.[9−12] Among block copolymers of three kinds, PEO−PPO, PEO−PPO−PEO, and PPO−PEO−PPO (where PEO and PPO are the abbreviations for poly(ethylene oxide) and poly(propylene oxide)), the type of PEO−PPO−PEO attracts more attention than the others.[13−17] The characterization methods reported on the aggregations of copolymers include NMR,[13−15] X-ray scattering,[16] DSC (differential scanning calorimetry) and SAXS (small-angle X-ray scattering),[4] and so on.[17,18]

Computer simulation is able to provide more microscopic-level information than experiment. The simulation methods often used are dissipative particle dynamics (DPD),[19−23] discontinuous molecular dynamics (DMD),[24] Monte Carlo simulations,[25] and Brownian dynamics simulations.[26,27] DPD, the mesoscopic method developed by Hoogerburgge and Koolman, is especially appropriate for the simulation of solutions of amphiphilic polymer.[28−30] DPD simulation technique can be used to investigate systems that contain millions of atoms.[31−36] The parameters used for carrying out DPD simulation can be obtained from the Flory−Huggins theory.[37] The elementary units in the DPD method are soft beads. A bead contains at least several molecules or molecular groups, but is still macroscopically small.[38] In our previous works, we had investigated aggregation behavior[39] and phase diagram[36] of surfactant systems and the interaction between surfactant and polymer.[32,40]

In the present paper, the aggregations of three block copolymers, $(EO)_{16}(PO)_{18}$, $(EO)_8(PO)_{18}(EO)_8$, and $(PO)_9(EO)_{16}(PO)_9$ in aqueous solution were simulated by the DPD method. The aim was to obtain the information on the aggregates formed by block copolymers with the same composition but different architecture. It had been found from these simulations that there were different aggregating behaviors as the concentration or structure of the copolymer was altered. The density distribution of beads and the end-to-end distance of copolymers could also provide important information about their aggregation.

2. Simulation Method

2.1. Theory. In the DPD method, the time evolution of the interacting particles is governed by Newton's equation of motion[34] as given in eqs 1a and 1b

$$\frac{d\vec{r}_i}{dt} = \vec{v}_i \tag{1a}$$

$$\frac{d\vec{v}_i}{dt} = \vec{f}_i \tag{1b}$$

where $\vec{r}_i, \vec{v}_i, \vec{f}_i$ are the position vector, the velocity, and the total force for the ith bead, respectively. All bead masses are set equal to unity for simplicity. In the DPD model, the total force of beads is given in eq 2[34]

$$F_i = \sum_{i \neq j} F_{ij}^{C} + \sum_{i \neq j} F_{ij}^{D} + \sum_{i \neq j} F_{ij}^{R} \tag{2}$$

* Corresponding author. Phone: +86-531-88365436. Fax: +86-531-88564750. E-mail: xuguiying@sdu.edu.cn.

10.1021/jp053636r CCC: $30.25
Published on Web 10/25/2005

where F_{ij}^{C} is a conservative force which is linear in the bead−bead separation, F_{ij}^{D} is a dissipative force which is proportional to the relative velocity of beads i and j, and F_{ij}^{R} is a random force between a bead i and its neighbor bead j. They are given by

$$F_{ij}^{C} = \begin{cases} \alpha_{ij}(1 - r_{ij})\hat{r}_{ij} & r_{ij} < 1 \\ 0 & r_{ij} > 1 \end{cases} \tag{3}$$

$$F_{ij}^{D} = \begin{cases} -\gamma\omega^{D}(r_{ij})(\hat{r}_{ij}\vec{v}_{ij}) & \hat{r}_{ij}r_{ij} < 1 \\ 0 & r_{ij} > 1 \end{cases} \tag{4}$$

$$F_{ij}^{R} = \begin{cases} \sigma\omega^{R}(r_{ij})\xi_{ij}\vec{r}_{ij} & r_{ij} < 1 \\ 0 & r_{ij} > 1 \end{cases} \tag{5}$$

where $r_{ij} = |\vec{r}_i - \vec{r}_j|$, $\hat{r}_{ij} = \vec{r}_{ij}/r_{ij}$ and where a_{ij} is the maximum repulsive force between particle i and particle j. Unlike the conservative force, the weight functions $\omega^{D}(r_{ij})$ and $\omega^{R}(r_{ij})$ of the dissipative forces and random forces couple together to form a thermostat. Espagnol and Warren[33] show the relations between the two functions

$$\omega^{D}(r) = [\omega^{R}(r)]^2$$

$$\sigma^2 = 2\gamma k_B T \tag{6}$$

where σ and γ are the two multiplicative constants which are related by temperature T, and T is the absolute temperature and k_B is the Boltzmann constant. For simplicity, a choice of $\omega^{D}(r)$ is taken as follows:

$$\omega^{D}(r) = [\omega^{R}(r)]^2 = \begin{cases} (1 - r)^2 & r < 1 \\ 0 & r \geq 1 \end{cases} \tag{7}$$

The Newtonian equation of position and velocity of particles is solved by a modified version of the velocity Verlet algorithm.[41] In the simulation, the radius of interaction, the particle mass, and the temperature were chosen as $r_c = m = kT = 1$ and $\sigma = 3.67$, while the particle density $\rho = 3$ (taking into account the computational efficiency, $\rho = 3$ is a reasonable choice). The only parameter to be determined is the maximum repulsive force a_{ij}, which is chosen according to the linear relation with Flory−Huggins χ parameters[37]

$$\alpha_{ij} \approx \alpha_{ii} + 3.27\chi_{ij} \text{ for } \rho = 3 \tag{8}$$

The χ parameter between DPD pairs of particles can be obtained from the calculation of the mixing energy with Blend module of Cerius 2. In Blend module, the interaction energies of mixing between different particles E_{mix} are calculated using the following equation:[42]

$$E_{mix}(T) = \frac{1}{2}\left(\sum_{i \neq j} Z_{ij}E_{ij}(T) - \sum_{i=j} Z_{ij}E_{ij}(T)\right) \tag{9}$$

where E_{ij} is the interaction energy of the complex composed of one molecule i and one molecule j, and Z_{ij} is the coordination number, i.e., the number of molecules j which can surround one molecule i in space. After the mixing energy of two particles has been calculated, the interaction parameter can be obtained via the following equation:[42]

$$\chi = Z \cdot V_{seg}\frac{E_{mix}(T)}{RT} \tag{10}$$

where Z denotes the average coordination number and V_{seg} is the volume of one polymer segment, while RT is the product of the gas constant and the Kelvin temperature. The interaction intensity between different molecules can be indicated by the interaction parameters.

The diffusion coefficient of a DPD particle is a dimensionless parameter characterizing the fluid and can be interpreted as the ratio between the time for fluid particles to diffuse a given distance and the time for hydrodynamic interactions to reach steady state on the same distance. The diffusion coefficient can be derived as follows:[34]

Focus on the equation of motion of a single particle and ignore the conservative forces.

$$\frac{dv_i}{dt} = \sum_{i \neq j} F_{ij}^{D} + \sum_{i \neq j} F_{ij}^{R} \tag{11}$$

The drag force is linear in the velocity difference, and thus, the part due to the motion of the ith particle may be separated out. Dropping the other part but retaining the random force gives a Langevin equation for the motion of the ith particle

$$\frac{dv_i}{dt} + \frac{v_i}{\tau} = F^{R} \tag{12}$$

where

$$\frac{1}{\tau} = \sum_{j \neq i} \gamma\omega^{D}(r_{ij})\frac{\hat{r}_{ij} \cdot \hat{r}_{ij}}{3}$$

$$F^{R} = \sum_{j \neq i} \sigma\omega^{R}(r_{ij})\xi_{ij}\hat{r}_{ij} \tag{13}$$

Replacing the sum for the drag factor by an integral, and likewise in the calculation of the statistics of the random force F^{R}, obtains

$$\frac{1}{\tau} = \frac{4\pi\gamma\rho}{3}\int_0^\infty dr\, r^2\omega^{D}(r)$$

$$\langle F^{R} \rangle = 0$$

$$\langle F^{R}(t) \cdot F^{R}(t') \rangle = 4\pi\sigma^2\rho \int dr\, r^2[\omega^{R}(r)]^2\delta(t - t') \tag{14}$$

The Langevin equation is solved straightforwardly, and therefore

$$D = \frac{1}{3}\int_0^\infty dt \langle v_i(0) \cdot v_i(t) \rangle = \tau k_B T \tag{15}$$

The fluctuation−dissipation theorem in this case takes the form

$$\sigma^2 \int_0^\infty dr\, r^2[\omega^{R}(r)]^2 = 2\gamma k_B T \int_0^\infty dr\, r^2\omega^{D}(r) \tag{16}$$

Inserting the expression for the dissipative function gives the diffusion coefficient

$$D = 45k_B T/2\pi\gamma\rho r_c^{\,3} \tag{17}$$

2.2. Simulation Parameters. Three kinds of copolymers $(EO)_{16}(PO)_{18}$, $(EO)_8(PO)_{18}(EO)_8$, and $(PO)_9(EO)_{16}(PO)_9$ were chosen in order to simulate the aggregation process of block copolymer with various structures in aqueous solution. Suppose we had a mixture of copolymer and water with the amounts n_p and n_w, and a total amount $n = n_p + n_w$ of the mixture. Then, the fraction n_p/n would be the relative amount of component

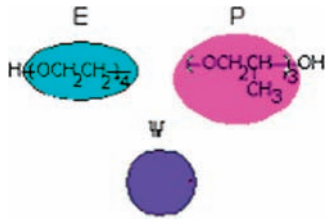

Figure 1. Schematic representation of block copolymer and water in DPD system.

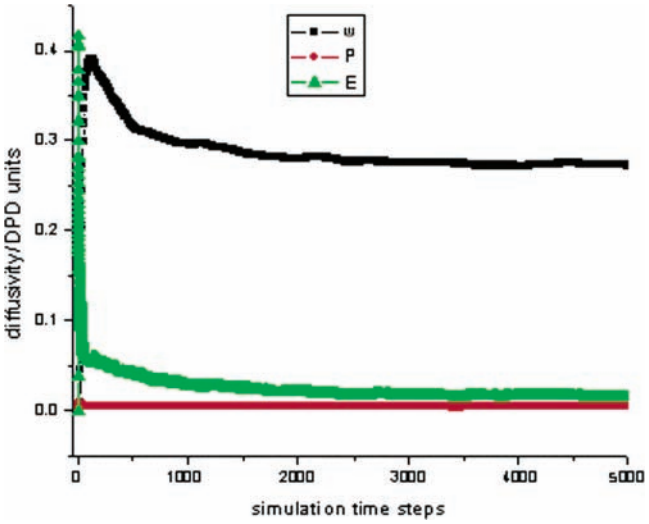

Figure 2. Diffusion plot of beads of $E_2P_6E_2$ with the simulation steps increasing at $x_p = 0.19$.

copolymer present, which would be called the molar fraction of copolymer and denoted x_p.

PPO, PEO, and water were represented by DPD beads P, E, and W as shown in Figure 1. According to the references,[8,43] one bead E represented four ethylene oxide molecules, one bead P represented three propylene oxide molecules, and one bead W represented one water molecule for convenience in Blend module of Cerius 2. So, three kinds of copolymers mentioned above were simply represented by E_4P_6, $E_2P_6E_2$, and $P_3E_4P_6$ in the simulation. Thus, copolymers were constructed by connecting the neighboring beads together via the harmonic springs $F_i^S = \sum_j Cr_{ij}$.[37] The spring constant was chosen as 4 according to ref 43. In the simulation, a 3D box of size $10 \times 10 \times 10$ with periodic boundary conditions was adopted. In Blend module, four ethylene oxide molecules, three propylene oxide molecules, and one water molecule were chosen as three units to calculate the E_{mix}, Z, and V_{seg}, in which several interactions were considered, such as hydrogen bond, van der Waals interaction, and so on. For example, the average coordination number Z_{WE} is 3.6, and the volume of V_E is 0.76 nm^3. Then, the interaction parameters between different beads obtained by eqs 9 and 10 were given in Table 1. At the simulation temperature, it could be deduced from the interaction parameter that bead E was more hydrophilic than P. The dissipative parameter γ was set to a value of 4.5 kT. The only length scale in the system was the cutoff radius r_c which was the length unit in the simulation. For each system, 20 000 time steps per simulation were carried out.

TABLE 1: Interaction Parameters a_{ij} (in DPD units) of the Simulation System

	E	P	W
E	25.00	48.87	35.93
P	48.87	25.00	38.32
W	35.93	38.32	25.00

3. Simulation Results and Discussion

With one diffusion plot (Figure 2) of the simulation results as an example, it could be seen that equilibrium was reached before 3000 time steps, so 20 000 time steps per simulation was sufficient for the simulation. It could be seen from Figure 2 that the diffusibility of bead E was better than that of bead P.

3.1. Morphology of Aggregates. The aggregates of $(EO)_{16}(PO)_{18}$ at different concentrations were shown in Figure 3. The red portion represented the hydrophobic bead P, the green one represented the hydrophilic bead E, and the water was neglected in all figures for clarity (the same for Figures 4−6). It was seen that diblock copolymer $(EO)_{16}(PO)_{18}$ could form spherical (Figure 3a), cylindrical (Figure 3b), intercluster micelle (Figure 3c), and lamellar phase (Figure 3d) with increasing concentration, and in addition, the aggregate sizes increased with increasing concentration. The hydrophilic EO chains were located outside, while the hydrophobic PO chains were located inside the aggregates.

The probable reasons for formation of spherical and cylindrical micelles were the hydrophobic interaction between the hydrophobic PO chains and the hydrogen bonds between EO

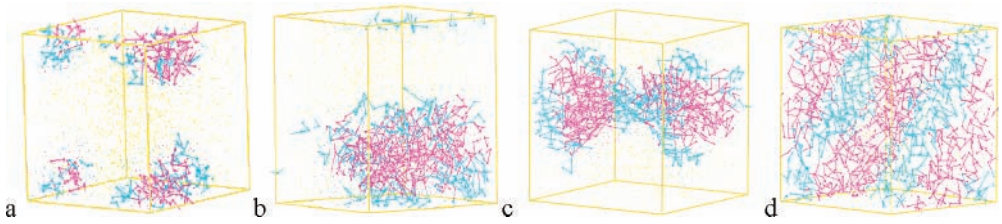

Figure 3. Snapshots of typical aggregates from simulation for $(EO)_{16}(PO)_{18}$ at different molar fractions.

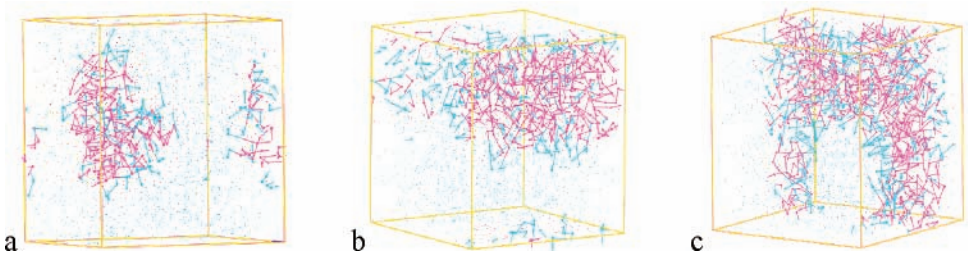

Figure 4. Snapshots of typical aggregates from simulation for $(EO)_8(PO)_{18}(EO)_8$ at different molar fractions.

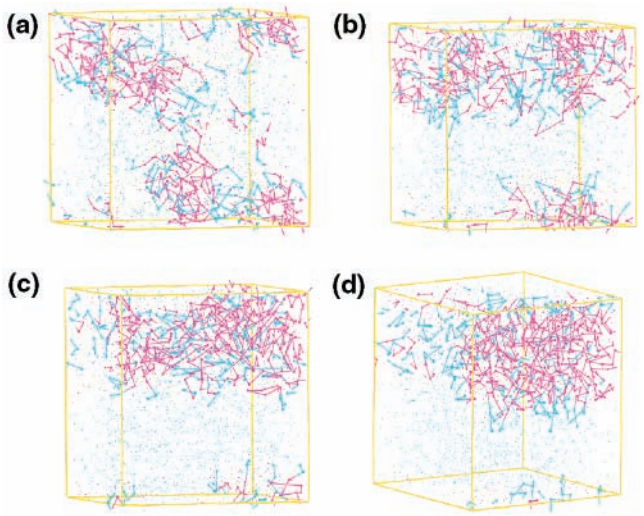

Figure 5. Aggregation evolution of $(EO)_8(PO)_{18}(EO)_8$ observed with the simulation steps increasing at $x_p = 0.19$. (a) 1000, (b) 2000, (c) 3000, and (d) 20 000 steps.

and water. The mechanism of the intercluster and lamellar phase formation may be that different aggregates shared the same hydrated layer. In the hydrated layer, hydrophilic chains of different aggregates formed hydrogen bonds with water, which were linked together by hydrogen bonds between water molecules. Thus, there were also two kinds of forces contributing to the formation of intercluster micelles and lamellar phase: hydrogen bonds between EO and water and between water and water of the hydrated layer; hydrophobic interaction between hydrophobic sections of different copolymer chains. The results agrees with those obtained from theory and experiment.[44]

Figure 4 showed the simulated results of $(EO)_8(PO)_{18}(EO)_8$ at different concentrations. Triblock copolymer $(EO)_8(PO)_{18}$-$(EO)_8$ could form spherical (Figure 4a) and cylindrical micelles (Figure 4b), as well as lamellar phase (Figure 4c) in aqueous solution with increasing concentration increasing. There had been no report on the formation of cylindrical micelles from triblock copolymers with hydrophilic ends and a hydrophobic middle block up to now. To understand the formation process of the cylindrical micelle well, the variation of the morphology of $(EO)_8(PO)_{18}(EO)_8$ aggregates with simulation time was shown in Figure 5 at the molar fraction $x_p = 0.19$: the copolymers started to form small aggregates with their hydrophobic chains attracted together by hydrophobic interaction as soon as the copolymers were added to water. Bigger aggregates formed by hydrophobic interaction when the hydrophobic chains of different small aggregates contacted other because of collision. The hydrophobic chains of large aggregates minimized their exposure to water as much as possible. On the contrary, the hydrophilic chains preferred contact with water molecules. So, aggregates readjusted to form cylindrical micelles.

The aggregates of copolymer $(PO)_9(EO)_{16}(PO)_9$ simulated at different molar fractions were shown in Figure 6. It was found that the spherical micelles (Figure 6a) formed at low concentrations. It was clearly seen that most of the copolymer chain adopted the loop shape (Figure 6b) with the end blocks of the copolymer chain aggregating together in the core and the hydrophilic middle block in contact with water. A few copolymer chains adopted extendible conformation. With the concentration increasing, intercluster micelles (Figure 6b) formed for the following reasons: different aggregates shared the same hydrated shell, just as the intercluster micelles formed by the diblock copolymer; middle blocks of the extendible triblock

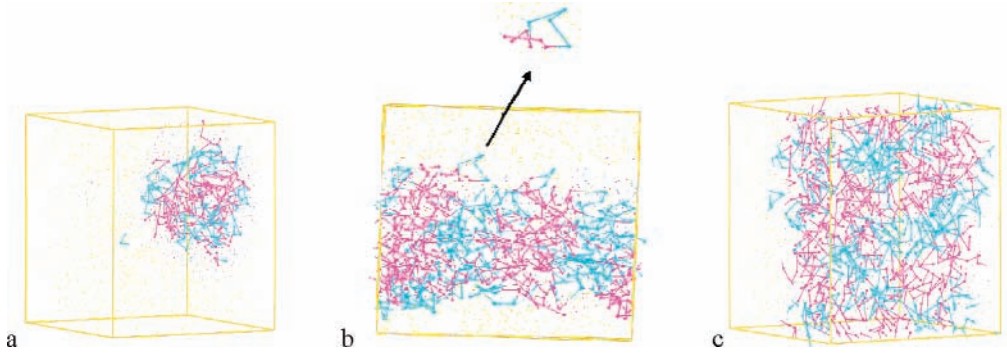

Figure 6. Snapshots of typical aggregates from simulation for $(PO)_9(EO)_{16}(PO)_9$ at different molar fractions.

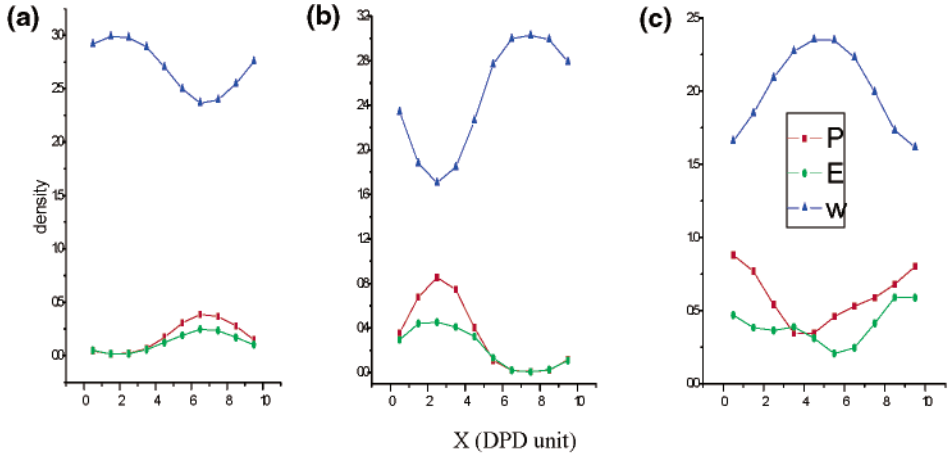

Figure 7. Density distribution of beads along *x* axis according to the different aggregates: the red line represents the density of P beads, green represents the E beads, and the blue line represent W beads.

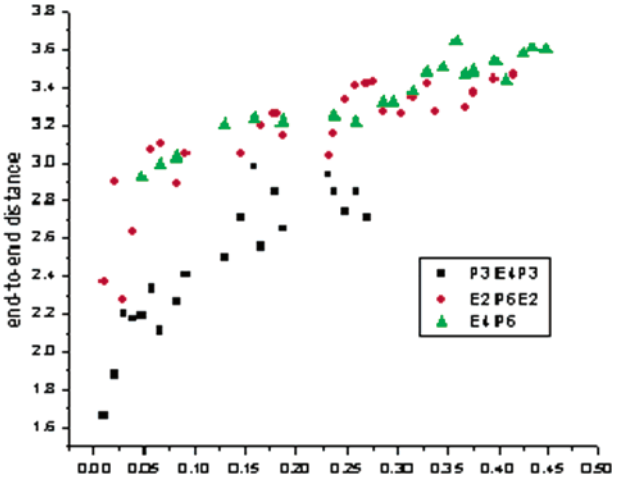

Figure 8. The end-to-end distance of block copolymers at different molar fractions.

copolymers bridged across different micelles, which led to attractive interactions between the micelles. When the concentration increased to a value ($x_p \geq 0.49$), the attractive interactions were strong enough to cause the formation of gels. Here, the gel formed at $x_p = 0.49$ was given as an example (Figure 6c).

3.2. Density Distribution of Beads. Figure 7 showed the density profile of aggregates of the three systems. It was clear that water penetrated to the whole aggregate. These results agreed with those of Won et al.[45] and Yang et al.[46] obtained from the experiment with SANS. Despite the fact that water swelled PEO chains, the hydrogen bond between them prevented possible phase transition, thereby making the micelles more stable. On the other hand, the presence of water between aggregates was one reason for the intercluster micelle and gel formation.

3.3. End-to-End Distance of Copolymers at Different Concentrations. The end-to-end distance was a concept derived from polymer science, which described the degree of curliness for a polymer chain. From Figure 8, it was obviously seen that the end-to-end distances increased with increasing concentration at the lower concentration region, indicating that copolymers were easily dissolved in water at low concentration. For all three copolymers, the size of different aggregates increased with the copolymer concentration, which made the end-to-end distances increase. The end-to-end distances of triblock copolymer $(EO)_8(PO)_{18}(EO)_8$ and diblock copolymer $(EO)_{16}(PO)_{18}$ were higher than that of $(PO)_9(EO)_{16}(PO)_9$, indicating that $(EO)_8$-$(PO)_{18}(EO)_8$ and $(EO)_{16}(PO)_{18}$ were more extendible than $(PO)_9(EO)_{16}(PO)_9$ in aqueous solution. For most of the triblock copolymer $(PO)_9(EO)_{16}(PO)_9$, the possible conformation was one in which the chain formed a loop-shaped structure with the two hydrophobic ends assembled together in the hydrophobic core while the hydrophilic middle was in contact with water molecules. A few $(PO)_9(EO)_{16}(PO)_9$ copolymers adopting an extendible conformation could be inferred from higher end-to-end distances. These extendible conformations attributed to the formation of intercluster micelles and gels.

4. Conclusion

Aggregates of three block copolymers with the same composition but different architecture were simulated. The simulation results indicated that the architecture and concentration of copolymer influenced the aggregate shape and size. All the three block copolymers would form spherical micelles at low concentration. However, with the concentration increasing, triblock $(EO)_8(PO)_{18}(EO)_8$ took cylindrical micelles and lamellar phase, diblock $(EO)_{16}(PO)_{18}$ tended to form cylindrical micelles, intercluster micelles, and lamellar phase, and triblock $(PO)_9$-$(EO)_{16}(PO)_9$ tended to form intercluster aggregates and gels. Different from the traditional aggregates formed by low molecular weight surfactants, aggregates formed by the three studied copolymers included a large amount of water. For diblock copolymer $(EO)_{16}(PO)_{18}$, intercluster micelles formed because different aggregates shared the hydrated shell. For triblock copolymer $(PO)_9(EO)_{16}(PO)_9$, intercluster micelles formed for two reasons: different aggregates shared the hydrated shell and the hydrophilic block acted as a bridge. In comparison with block copolymer $(PO)_9(EO)_{16}(PO)_9$, the other two copolymers adopted more extendible conformations in aqueous solution. The simulation results also showed that bead E diffused more rapidly than bead P.

Acknowledgment. We would like to acknowledge financial support for this work by the National Natural Scientific Foundation (20573067, 20303011) and National Science Foundation (Y2004B06) of Shandong Province in China.

References and Notes

(1) Ivanova, R.; Lindman, B.; Alexandridis, P. *Adv. Colloid Interface Sci.* **2001**, *89*, 351.
(2) Ye, X.; Wu, J.; Oh, J. K.; Winnik, M. A.; Wu, C. *Macromolecules* **2003**, *36*, 8886.
(3) Brandani, P.; Stroeve, P. *Macromolecules* **2003**, *36*, 9492.
(4) Ishoy, T.; Mortensen, K. *Langmuir* **2005**, *21*, 1766.
(5) Lisi, R. D.; Lazzara, G.; Milioto, S.; Muratore, M. *J. Phys. Chem. B* **2004**, *108*, 18214.
(6) Varade, D.; Bahadur, P. *Tenside, Surfactants, Deterg.* **2002**, *39* (2), 48−52.
(7) Wang, R.; Knoll, H.; Rittig, F.; Karger, J. *Langmuir* **2004**, *17*, 7464.
(8) Lam, Y. M.; Goldbeck-Wood, G.; Boothroyd, C. *Mol. Simul.* **2004**, *30*, 239.
(9) Mata, J.; Joshi, T.; Varade, D.; Ghosh, G.; Bahadur, P. *Colloids Surf., A* **2004**, *247*, 1.
(10) da Silva, R. C.; Loh, W. *J. Colloid Interface Sci.* **1998**, *202*, 385.
(11) Contractor, K.; Bahadur, P. *Eur. Polym. J.* **1998**, *34*, 225.
(12) Varade, D.; Sharma, R.; Aswal, V. K.; Goyal, P. S.; Bahadur, P. *Eur. Polym. J.* **2004**, *40*, 2457.
(13) Sadaghiani, A. S.; Khan, A.; Lindman, B. *J. Colloid Interface Sci.* **1989**, *132*, 352.
(14) Sadaghiani, A. S.; Khan A. *Langmuir* **1991**, *7*, 898.
(15) Khan, A.; Zhang, K. W.; Mendonca, C. *J. Colloid Interface Sci.* **1994**, *165*, 253.
(16) Funari, S. S.; di Vitta, C.; Rapp, G. *Acta Phys. Pol., A* **1997**, *91*, 953.
(17) Rassing, J.; Attwood, D. *Int. J. Pharmacol.* **1983**, *13*, 47.
(18) Zhou, Z.; Chu, B. *Macromolecules* **1987**, *20*, 3089.
(19) Morozov, A. N.; Fraaije, J. G. E. *Macromolecules* **2001**, *34*, 1526.
(20) Malfreyt, P.; Tildesley, D. J. *Langmuir* **2000**, *16*, 4372.
(21) Groot, R. D.; Madden, T. J.; Tidesley, D. J. *J. Chem. Phys.* **1999**, *110*, 9739.
(22) (a) Leibler, L.; Pakula, T.; Karatasos, T. *Macromolecules* **1980**, *13*, 1602. (b) Pakula, T.; Anastasiadis, S. H.; Fytes, G. *Macromolecules* **1997**, *30*, 8463.
(23) Shillcock, J. C.; Lipowsky, R. *Chem. Phys.* **2002**, *117*, 5048.
(24) Schultz, A. J.; Hall, C. K.; Genzer, J. *J. Chem. Phys.* **2002**, *117*, 10329.
(25) Yuan, S. L.; Xu, G. Y.; Cai, Z. T. *J. Colloid Polym. Sci.* **2003**, *281*, 66.
(26) Pastor, R. W.; Venable, R. M.; Karplus, M.; Szabo, A. *J. Chem. Phys.* **1988**, 89.
(27) (a) Nagochi, H. *J. Chem. Phys.* **2002**, *117*, 8130. (b) Nagochi, H.; Takasu, M. *J. Chem. Phys.* **2001**, *115*, 9547.
(28) Hoogerbrugge, P.; Koolman, J. *Europhys. Lett.* **1992**, *19*, 155.
(29) Groot, R. D.; Madden, T. J. *J. Chem. Phys.* **1998**, *108*, 8713.
(30) Qian, H. J.; Lu, Z. Y.; Chen, L. J.; Li, Z. S.; Sun, C. C. *Macromolecules* **2005**, *38*, 1395.
(31) Misselyn Bauduin, A. M.; Thibaut, A.; Grandjean, J.; Broze, G.; Jerome, R. *Langmuir* **2000**, *16*, 4430.
(32) Li, Y. M.; Xu, G. Y.; Luan, Y. X.; Yuan, S. L.; Zhang, Z. Q. *Colloid Surf., A* **2005**, *385*, 257.

(33) Espagnol, P.; Warren, P. *Europhys. Lett.* **1995**, *30*, 191.
(34) Groot, R. D.; Wrren, P. B. *J. Chem. Phys.* **1997**, *107*, 4423.
(35) (a)Ryjkina, E.; Kuhn, H.; Rehage, H.; Muller, F.; Peggau, J. *Angew. Chem.* **2002**, *114*, 1025. (b) Ryjkina, E.; Kuhn, H.; Rehage, H.; Muller, F.; Peggau, J. *Angew. Chem., Int. Ed.* **2002**, *41*, 983.
(36) Yuan, S. L.; Cai, Z. T.; Xu, G. Y.; Jiang, Y. S. *J. Chem. Phys. Lett.* **2002**, *365*, 347.
(37) Flory, P. *Principles of Polymer Chemistry*; Cornell University Press: Ithaca, NY, 1953; p 12.
(38) Shillcock, J. C.; Lipowsky, R. *J. Chem. Phys.* **2002**, *117*, 5048.
(39) Yuan, S. L.; Cai, Z. T.; Xu, G. Y. *Chin. J. Chem.* **2003**, *21*, 112.
(40) Yuan, S. L.; Cai, Z. T.; Xu, G. Y.; Jiang, Y. S. *Colloid Polym. Sci.* **2003**, *281*, 1069.
(41) Martys, N. S.; Mountain, R. D. *Phys. Rev. E* **1999**, *59* (3) 3733−3736.
(42) Blanco, M. J. *Comput. Chem.* **1991**, *12*, 237.
(43) Li, Y. Y.; Hou, T. J.; Guo, S. L.; Wang, K. X.; Xu, X. J. *Phys. Chem. Phys.* **2002**, *2*, 2749.
(44) Leist, H. *J. Chem. Phys.* **1999**, *110*, 639.
(45) Won, Y. Y.; Davis, H. T.; Bates, F. S.; Agmalian, M.; Wignall, G. D. *J. Phys. Chem. B* **2000**, *104*, 7134.
(46) Yang, L.; Alexandridis, P.; Steytler, D. C.; Kositza, M. J.; Holzwarth, J. F. *Langmuir* **2000**, *16*, 8555.